Repulsion from slow-diffusing nutrients improves chemotaxis towards moving sources

Blox Bloxham, Hyunseok Lee, Jeff Gore

Abstract

Chemotaxis, or the following of chemical concentration gradients, is essential for microbes to locate nutrients. A microbe can swim in the direction of increasing nutrient concentrations to reach the source. However, microbes often display paradoxical behaviors, such as *Escherichia coli* being repulsed by several amino acids. Here, we explore chemotaxis towards a moving target and demonstrate that repulsion from a nutrient can actually improve chemotaxis towards its source. Because a moving source leaves most of the nutrient plume behind it, simply following the concentration gradient produces inefficient intercept trajectories. However, when attraction to a fast-diffusing molecule and repulsion from a slow-diffusing molecule are combined, motion in a new direction emerges and intercept times are significantly reduced. When the source is moving faster than the microbe can swim this differential strategy can even be essential to ever intercepting the source at all. Finally, we leverage existing data to show that *E. coli* is attracted to fast-diffusing amino acids and repulsed by slow-diffusing ones, suggesting it may utilize a differential strategy and providing a possible explanation for its repulsion from certain amino acids. Our results thus illuminate new possibilities in how microbes can integrate signals from multiple concentration gradients and propose a new strategy by which microbe may accomplish the difficult task of intercepting a moving target.

Introduction

The ability to gather nutrients is essential for any organism to grow. In a spatially heterogeneous world, the acquisition of nutrients can be greatly improved by moving towards locations with the most favorable conditions[1–3]. For microbes, this generally involves following chemical gradients towards increasing concentrations of attractants and

away from increasing concentrations of repellants, a behavior known as chemotaxis[2,4–11]. Attractants can be nutrients diffusing from their source[12,13] or other indicators of favorable conditions[6]. Repellants are often, but not always[14], toxins or other harmful compounds or conditions[14–16]. Chemotaxis is essentially a gradient ascent: to find the highest nutrient concentration, microbes simply move in whichever direction it's locally increasing.

Microbes do, however, display surprising patterns as to which compounds are attractants and which are repellants. For example, *Escherichia coli* is repelled by certain amino acids[14,16] including some it can utilize as food[16], as well as other nutrients such as glycerol[17] and even combinations of attractants[18]. A recent investigation demonstrated that many of the amino acids *E. coli* is repelled by are less effective nutrients for it and in some cases inhibit growth[16]. Anomalies do remain, however, such as tryptophan being one of the amino acids that supports the most growth as the sole nitrogen or nitrogen and carbon source but also being the strongest repellant[16]. Other surprising chemotactic responses include *Pseudomonas aeruginosa* being attracted to lethal antibiotics such as ciprofloxacin and streptomycin, possibly as a strategy to target and invade competing colonies[19]. Microbes have also been observed to be sometimes attracted to and sometimes repelled by the same compounds, depending on concentration and other factors[20]. *E. coli's* repulsion from nutrients and these other intriguing results illustrate how microbes may be integrating external signals in sophisticated ways to carefully tune their trajectories.

Natural sources of chemoeffectors (attractants and repellents) will generally be sources of more than one, and the resulting presence of multiple concentration gradients creates additional opportunities for sophisticated signal processing. When faced with two opposing attractant gradients microbes must choose between the two, with outcomes potentially dependent on previous environmental exposure and resulting receptor expression[21–23]. In the presence of parallel attractant and repellant gradients, microbes must make a similar choice between net attraction or repulsion[24–29], with chemotaxis to an intermediate distance from the source or a 'bet-hedging' split into attracted and repelled subpopulations also being possible outcomes[25]. In some cases, a microbe will only respond to one chemoeffector if another is present[18]. On the broader theme of chemotaxis in realistically complex

environments, the combination of faster growth on a colony's edge and chemotaxis towards compounds secreted during growth can significantly boost range expansion[30,31]. However, while recent research has illuminated the importance of carefully considering spatial structure when exploring chemotaxis, previous reports appear to have only considered chemoeffector gradients that are roughly parallel or antiparallel, leaving the effect of combining nonparallel gradients largely unexplored. More broadly, how the surprising chemotactic behaviors of microbes and the integration of multiple signals come together to solve complex, real-world navigation tasks presents exciting opportunities for exploration.

In addition to being spatially structured, the world is in constant motion, so chemotaxis will often involve intercepting a moving source. An important example is marine microbes intercepting sinking particulate organic matter (marine snow), where rates of successful intercept have important implications for the global carbon cycle[32]. These particles are often sinking faster than the microbe can swim[33–35], so small differences in trajectory can make the difference between a successful intercept and getting stuck behind unable to ever catch up[36]. Chemotaxis towards a moving source could also take the form of one microbe trying to intercept another for the purposes of predation or cross feeding[37,38]. A stationary source surrounded by a fluid flow is also an equivalent scenario under a change in reference frame[39,40]. Thus, it is essential to consider the performance of chemotactic strategies in the case of a moving source to fully understand nutrient acquisition in natural environments, and doing so may yield insight into the observed complexities of chemotactic behavior.

Here, we demonstrate how repulsion from a nutrient can actually improve chemotaxis towards a moving source. Specifically, we present a simple differential strategy that combines attraction to a fast-diffusing molecule and repulsion from a slow-diffusing one to significantly outperform any purely attractive strategy at intercepting a moving source. We further show this differential strategy can even make the difference as to whether a fast-moving source is ever intercepted at all. We conclude by highlighting that *E. coli* is attracted to fast-diffusing and repelled by slow-diffusing amino acids – exactly as needed to implement this strategy. Our results thus present a novel mechanism for microbes to accomplish a difficult task and suggest an explanation for surprising experimental observations.

Results

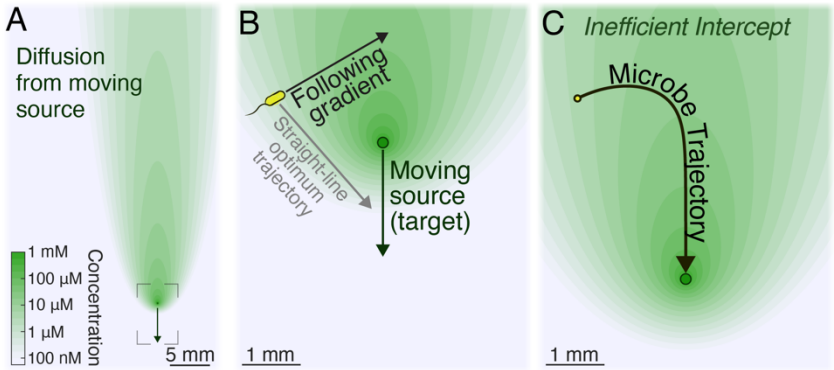

Figure 1. Inefficiency of following an attractant gradient to intercept a moving source. (**A**) Concentration profile of a molecule with diffusion coefficient 1000 $\mu m^2/s$ being released from source (represented by the small dot above the arrow) moving downwards at 5 µm/s. (**B**) Zoomed in view of the region of **A** highlighted by the dashed box with a cartoon microbe and arrow indicating the direction of the gradient of the concentration at an example point at the center of the microbe's body. Light gray line indicates the direction the microbe would need to travel in to most efficiently intercept the source if it could follow any trajectory. (**C**) Trajectory that a microbe starting at the example point in **B** would follow to intercept the moving source if it followed the gradient of the attractant. Drawn in the same stationary frame as **B** at the moment the source is intercepted.

Following the gradient of an attractant is inefficient for intercepting a moving target. We began by benchmarking the difficulty of intercepting a moving target via chemotaxis. We modeled a point source moving at constant velocity and releasing a chemoeffector at a constant rate. This could, for example, be a model of marine snow or other sinking particulate matter with the majority of relevant swimming happening far enough from the particle that local fluid flows can be ignored. As the source is in constant motion, it leaves a tail of

chemoeffector behind, as the molecules diffuse from past locations of the source (Fig. 1A). The concentration lagging behind the source means the gradient points behind and even net away from the source at most locations such that a microbe following this gradient is not swimming towards the source (Fig 1B). Moreover, the optimal intercept trajectory is to aim ahead of the source at its future location, which further increases the discrepancy between following the chemical gradient and the optimal direction of travel (Fig 1B). Thus, the basic geometry appears to make intercepting a moving target via chemotaxis an inherently difficult task.

We proceeded to simulate trajectories of microbes following the simple strategy of swimming in the direction of increasing chemoeffector concentration. We chose a deterministic approximation in which the microbe swam exactly in the direction of the concentration gradient with no explicit run-and-tumble (under which a microbe would alternate 'tumbling' to reorient into a new direction and 'running' for a variable distance) or other stochastic motion. (We reproduce our key results with stochastic run-and-tumble motion in Appendix §5.) We set the microbe velocity to 10 μm/s (an approximate to slightly high net velocity for *E. coli* after averaging over runs and tumbles[41]) and the source velocity to 5 μm/s. We considered a "fast-diffusing" chemoeffector with diffusion coefficient 1000 $\mu m^2/s$ and a "slow-diffusing" chemoeffector with diffusion coefficient 500 $\mu m^2/s$ (roughly spanning the range of coefficients for amino acids). The microbe intercepted the source by coming within 100 μm. Following either the fast-diffusing or the slow-diffusing chemoeffector produced trajectories that initially aimed behind and away from the source before finally turning towards the source once the microbe was almost directly behind it (Fig 1C and Appendix Fig S1B). Across a range of initial positions, it frequently took the microbe nearly twice as long to intercept the source than if it could follow an optimal straight-line intercept trajectory (Appendix Fig S2). Thus, there exists significant room for improvement over simply following the gradient of an attractant to reach a moving source.

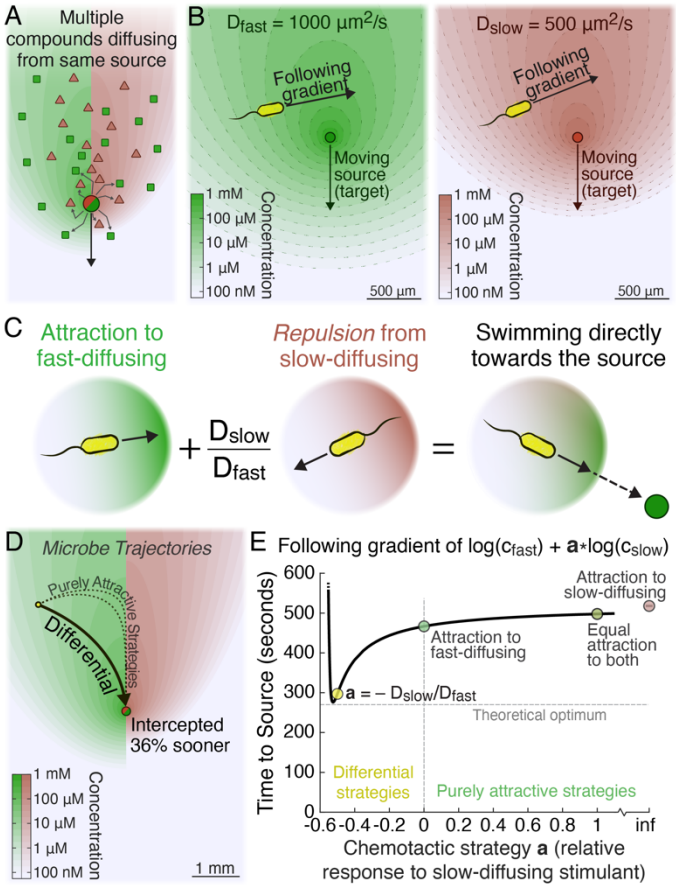

Figure 2. Combining attraction and repulsion outperforms purely attractive chemotaxis at intercepting a moving source. (**A**) Cartoon illustrating multiple chemoeffectors being released from the same source. (**B**) Comparison of the gradients of the fast-diffusing chemoeffector (left) and slow-diffusing chemoeffector (right) being release by a source moving at 5 μm/s. Directions of the concentration gradients at the center of the microbe bodies are illustrated with arrows. (**C**) Visual definition of the differential strategy in which the same slow-diffusing chemoeffector is now treated as a repellant. With an appropriate weighting of the two signals (Results, Methods), the combined effect is motion directly towards the source. (**D**) Trajectory produced by the differential strategy (thick line) compared to following the gradients of the individual chemoeffector concentrations (thin dashed lines) for a microbe starting at the same example point as Figure 1B-C. The concentration of the fast-diffusing chemoeffector is shown on the left and the slow-diffusing on the right for visual clarity but both are present on both 'sides' as an azimuthal symmetry is assumed (Methods). (**E**) Time to reach the source from the same example point as **D** for a generalized differential strategy in which the relative response to the slow-diffusing chemoattractant is now a function of variable $\boldsymbol{a}$. Vertical dashed line separates the different strategies in which the slow-diffusing chemoeffector is used as a repellant (negative $\boldsymbol{a}$) from the strategies in which both chemoeffectors are attractants (positive $\boldsymbol{a}$). Horizontal dashed line represents the fastest the microbe could possibly reach the source if it could follow any straight-line trajectory. (Plot reproduced for additional starting point in Appendix Figure S4.)

Combining attraction to a fast-diffusing molecule and repulsion from a slow-diffusing molecule significantly reduces intercept times.

We next considered how a microbe might intercept a moving source more efficiently than is allowed by simply following the gradient of an attractant. In particular, we explored how signals from two chemoeffectors might be combined as there will typically be multiple molecules (with different diffusion coefficients) simultaneously being released by any real source (Fig 2A). We noted that, while the gradient of the fast-diffusing chemoeffector points slightly closer to the source than the gradient of the slow-diffusing chemoeffector (Fig 2B), the gradient of the slow-diffusing chemoeffector nevertheless contains useful information. Specifically, because the directions of the concentration gradients for fast- and slow-diffusing molecules point in different directions, a weighted sum or difference could therefore be constructed to point in any desired direction (within the relevant 2D cross-section). Upon inspecting the functional form of the spatial concentrations, we observed that the gradient of $\log[c_{\text{fast}}] - \left(\frac{D_{\text{slow}}}{D_{\text{fast}}}\right)\log[c_{\text{slow}}]$ (where c_{fast} and c_{slow} are the spatial concentrations of the fast- and slow-diffusing molecules and D_{fast} and D_{slow} are their diffusion coefficients) always points directly towards the source (Fig 1C, Methods). (In Appendix §4 we reproduce key results using a model directly based characterizations of *E. coli*.) Swimming directly towards the source is clearly a superior strategy than initially swimming away from it, so this differential strategy presents an opportunity for the microbe to significantly reduce the time needed to intercept the source.

To quantify just how much more efficiently the differential strategy allows a microbe to intercept a moving target, we reran our simulations with a microbe obeying this differential strategy. As an example, a microbe starting at the example point illustrated in Figures 1B, 1C, and 2D (Methods) intercepts the source 36% faster when following the differential strategy than when simply following an attractant gradient (Fig 2D, Appendix Fig S1B-D). Indeed, the differential strategy outperformed the purely attractive strategy for any initial position (except the trivial case of starting directly underneath; data later presented as part of Fig 3B). Thus, this simple differential strategy robustly reduces the time for a microbe to intercept a moving source.

This differential strategy in which the microbe swims directly towards the current location of the source is not necessarily, however, the optimal strategy since the source is still moving and an optimal trajectory would be to aim ahead of it at its future location. There is therefore potential room for improvement (about 10% for the example starting point used in the figures), so we explored whether an alternative strategy could do better. We varied the relative response to the slow-diffusing molecule by generalizing the strategy to one in which the microbe now followed the gradient of $\log[c_{\text{fast}}] + \boldsymbol{a}\log[c_{\text{slow}}]$ where $\boldsymbol{a}$ is a variable parameter with $\boldsymbol{a} = -\frac{D_{\text{slow}}}{D_{\text{fast}}}$ being the previously presented strategy. As repulsion from the slow-diffusing molecule was strengthened beyond $\boldsymbol{a} = -\frac{D_{\text{slow}}}{D_{\text{fast}}}$, the time to reach the source did indeed continue to decrease with a minimum at $\boldsymbol{a} \approx -1.05 * \frac{D_{\text{slow}}}{D_{\text{fast}}}$ for the example starting point (Fig 2E and Appendix Fig S3C for trajectory). Beyond this minimum, however, the time to source rapidly increased as repulsion was further strengthened (Fig 2E). By $\boldsymbol{a} = -1.12 * \frac{D_{\text{slow}}}{D_{\text{fast}}}$, trajectories no longer reached the source at all. When we varied the initial starting position, we observed that the further away from the source the microbe started the closer to $\boldsymbol{a} = -\frac{D_{\text{slow}}}{D_{\text{fast}}}$ the cutoff at which trajectories no longer reached the source became (Appendix Fig S4). Thus, $\boldsymbol{a} = -\frac{D_{\text{slow}}}{D_{\text{fast}}}$ emerged as the best strategy that never prevented the microbe from reaching the source due to repulsion being too strong. It therefore appears that the simple differential strategy with $\boldsymbol{a} = -\frac{D_{\text{slow}}}{D_{\text{fast}}}$ is a robust choice for a microbe to implement and a both simple and relevant strategy for our exploration to be benchmarking.

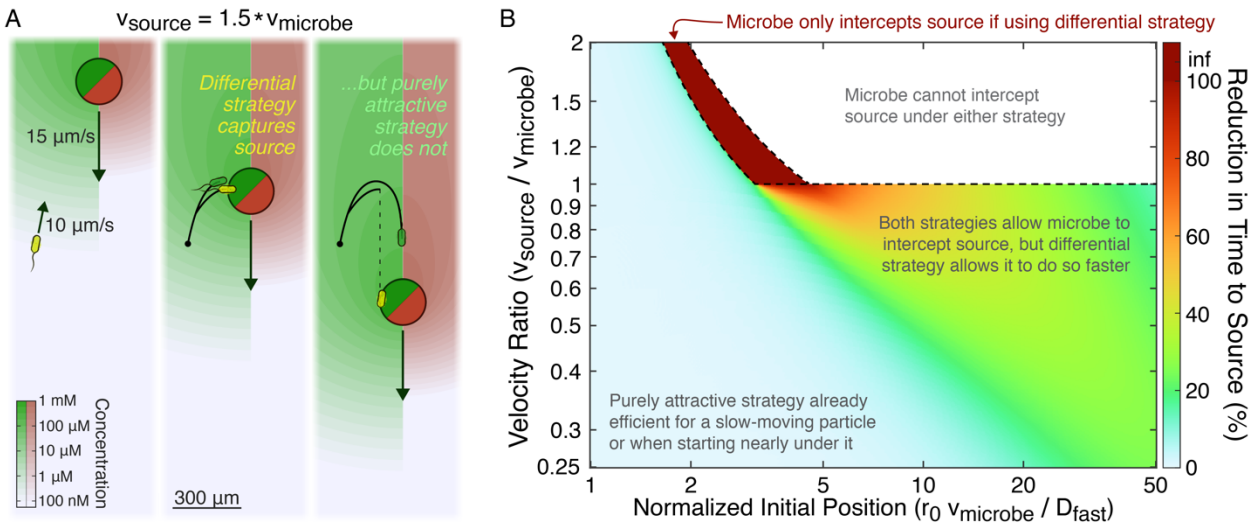

Figure 3. The differential strategy can even make the difference as to whether the source is ever intercepted at all and always outperforms purely attractant chemotaxis. (**A**) Illustration of a case in which the differential strategy allows the microbe to intercept the source when purely attractive chemotaxis would not. The same stationary frame is shown in each panel. The green microbe always follows the gradient of the fast-diffusing attractant while the yellow microbe implements the differential strategy once the concentration of the slow-diffusing repellant is above 100 nM. (**B**) Reduction in time for the microbe to reach the source for the differential strategy compared to following the gradient of the fast-diffusing chemoeffector as a function of the two most relevant dimensionless parameters (Results, Methods). White region in top right indicates conditions for which neither strategy is capable of intercepting the source. Adjacent dark red region indicates conditions for which only the differential strategy allows the microbe to intercept the source.

For a source moving faster than the microbe can swim, a differential strategy can make the difference as to whether it is ever intercepted at all.

Intercepting a food source sooner provides an obvious fitness benefit, but there are scenarios in which the microbe even being able to ever intercept it at all (after any amount of time) is uncertain, with the difference between intercepting and never intercepting being the vastly larger fitness difference. One scenario in which a microbe may fail to intercept a source is if the source is moving faster than it can swim[33,36]. For a faster moving source, the microbe must rapidly adjust its trajectory to intercept the source before it has passed or else it will never be able to catch up. The earlier and more pronounced downturn produced by

the differential strategy could therefore make a significant difference in intercept probabilities. Indeed, the differential strategy can allow the microbe to intercept a source moving faster than it can swim while purely attractive chemotaxis does not (Fig 3A). Thus, implementing a differential strategy can make the difference between proliferation and starvation if food sources are likely to be moving faster than the microbe can swim.

Having now explored specific examples of the two qualitatively distinct scenarios of a source moving either slower or faster than the microbe can swim, we proceeded to quantify the benefit of the differential strategy across a wide range of conditions. The two key dimensionless parameters controlling the time to intercept the source are the normalized initial position ($r_0 * v_{\mathrm{microbe}}/D_{\mathrm{fast}}$) and the velocity ratio $v_{\mathrm{source}}/v_{\mathrm{microbe}}$. We simulated trajectories across a range of initial positions and velocity ratios (Methods, Appendix Fig S5). From these trajectories, we calculated the reduction in time to source obtained by following the differential strategy compared to purely attractive chemotaxis (Fig 3B). As expected, the differential strategy always outperformed the purely attractive strategy (Fig 3B). When the microbe started nearly directly under the source or when the source was traveling slowly the improvement was small (Fig 3B). However, for microbes starting further away and a source moving closer to the microbe's swim speed there exists a broad region with improvements in the range of 25% to 50% and convergence towards 100% as the source velocity approached the microbe velocity (Fig 3B). For velocity ratios uniformly distributed from 0.25 to 1 and initial positions uniformly distributed on a disk of radius $50 * D_{\mathrm{fast}}/v_{\mathrm{microbe}}$, the average reduction in time to source was 26%. When the source was traveling faster than the microbe could swim, a significant region existed in which only the differential strategy allowed the microbe to intercept the source (Fig 3B). For the source traveling just slightly faster than the microbe could swim, the disk of initial positions from which the microbe could intercept the source was more than 2.5 times as large under the differential strategy than for purely attractive chemotaxis (Appendix Fig S6). Thus, implementing a differential strategy appears to provide a consistent and significant fitness benefit to a microbe trying to intercept a moving source.

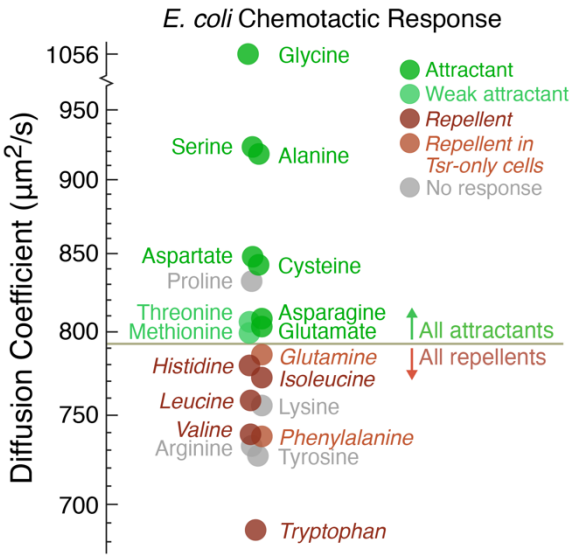

Figure 4. *E. coli* is attracted to fast-diffusing amino acids and repelled by slow-diffusing amino acids. Diffusion coefficients of the amino acids (vertical axis, Methods for source) along with *E. coli*'s chemotactic response as reported by Yang 2015[16] (colors). Amino acids that were described by Yang as weak attractants are colored separately as are amino acids that were only repellents to Yang's Tsr-only *E. coli*. Horizontal line separating attractants from repellents is an empirical observation based on data.

***E. coli* is attracted to fast-diffusing amino acids and repelled by slow-diffusing amino acids, as would be necessary for it to implement the differential strategy.**

Having shown the theoretical potential of a differential strategy, we proceed to establish a connection to existing experimental data. A thorough characterization of which amino acids are attractants and repellants for *E. coli* was performed by Yang 2015[16]. We used characterizations of MG1655 *E. coli* from this paper and compared to diffusion coefficients for each amino acid (Methods). A striking trend emerged in which all 9 attractants had diffusion coefficients greater than 790 $\mu m^2/s$ and all 5 repellants had diffusion coefficients less than this cutoff (Fig 4). This attraction to fast-diffusing amino acids and repulsion from slow-diffusing amino acids is exactly what would be needed to implement the differential strategy, suggesting *E. coli* may follow this strategy when trying to intercept a moving source of amino acids. In Appendix §4, we further demonstrate that competitive binding of attractive and repulsive amino acids to the Tsr receptor should allow *E. coli* to follow trajectories that closely match those produced by the differential strategy. Thus, in addition to the theoretical benefits of differential chemotaxis, there is evidence that microbes may actually be implementing this strategy as well as a new explanation for why *E. coli* would be repelled by certain nutrients.

Discussion

In this paper we demonstrate that a differential strategy combining attraction to fast-diffusing molecules with repulsion from slow-diffusing molecules can significantly improve chemotaxis towards a moving source. Employing this strategy can even make the difference as to whether the source is ever intercepted at all. We observed that *E. coli* is attracted to the fast-diffusing amino acids but repulsed by the slow diffusing ones (Fig. 4). In Appendix §4, we show that a model *E. coli's* Tsr receptor and its effect on CheA activity predicts trajectories that closely resemble those produced by the simple differential strategy, including in the presence of several attractants and repellants. There are other convincing explanations why *E. coli* would be repulsed to certain amino acids, in particular the correlations to utility as a nutrient and growth inhibition explored in Yang 2015[16], but ultimately multiple explanations for this behavior can be simultaneously true as traits can be beneficial for multiple reasons. Additionally, the specific example of repulsion to tryptophan is intriguing as it does not inhibit growth even at high concentrations[16] and can be utilized as *E. coli's* sole carbon and nitrogen source[16]. However, tryptophan is the slowest diffusing amino acid, which makes repulsion from it especially beneficial under the differential chemotaxis explanation. The benefits of differential chemotaxis therefore help explain some of the mystery behind *E. coli's* repulsion from certain amino acids.

We considered deterministic trajectories throughout the Main Text, but microbial motion is stochastic, so we extend our results with stochastic modeling in Appendix §5. In particular, microbes do not perfectly follow gradients but instead display run-and-tumble motion in which they "run" in a roughly straight line and then randomize their orientation by tumbling in response to worsening conditions before starting another run[10]. Over large enough distances and enough runs and tumbles, net motion does, however, closely match our deterministic approximation (Methods, Appendix §5). Thus, the benefits of differential chemotaxis are robust to this major source of real-world stochasticity.

Our calculations used a point-source calculation of concentration profiles and ignored the effects of turbulence, so it is important to determine in which regimes these calculations are valid. For a spherical particle, Kiørboe 2001[42] showed that if the particle is large and fast-moving relative to the diffusion coefficients of the relevant chemoeffectors (i.e. if it has a large Peclet number) then the concentration profile becomes long and narrow and likely poorly suited to realizing the benefits of differential chemotaxis. Thus, differential chemotaxis will be most applicable in cases of relatively small and slow-moving particles (or when attempting to intercept another microbe), as we studied here by using parameters that give Peclet numbers around 1. Regarding turbulence, Bachelor and Kolmogorov length scales can, for example, be up to hundreds of micrometers and tens of millimeters in the ocean thermocline[2]. Above these scales, turbulence becomes significant and any concentration profile will lose its shape[2]. This mixing means a microbe starting too far away is unlikely to reach the source under any strategy and also that it is possible to fall too far behind a source to catch back up even when the source is moving slowly. Thus, these fluids-based considerations largely limit to relevance of differential chemotaxis to cases where strategy can make the difference as to whether the source is ever intercepted at all – which is also when the potential fitness benefit is the largest.

The fluid flows close to a particle have the potential to affect not only the chemoeffector concentrations but also directly impact the microbe trajectories. Słomka 2020[36] provides a detailed account of how fluid flows around a particle impact microbe trajectories. Some of these effects could amplify the benefit of using a differential strategy to intercept a fast-moving source. Specifically, hydrodynamic screening and the effect of fluid strain on microbe orientation[36] largely eliminate the region of initial positions in which the microbe would intercept the particle regardless of strategy. Meanwhile, a microbe starting further away and approaching from the side experiences a strain-induced torque towards vertically upwards or downwards[36] that makes it crucial to be pointing sufficiently downwards upon entering the relevant region – which the earlier downturn of the differential strategy would provide. That sinking particles are likely irregular non-spherical shapes with both solid and mucus components should also be considered[43,44]. Detailed calculations of differential and purely attractive strategies with fluid flows and their effects on microbe trajectories should be

performed by future works, but it appears likely the benefits of differential chemotaxis will be robust to these corrections.

Another important direction for future work will be to experimentally characterize trajectories. A variation on the microfluidic chip used in Stocker 2008[33], in which an attractant was injected upstream of a cylindrical pillar surrounded by a fluid flow to simulate release from a sinking particle, might provide a nice experimental demonstration. An alternative system in which differential strategies could be explored is in surface-adhered bacteria. If the source is also fixed to the surface with a fluid flow elongating the concentration profiles, the differential strategy becomes the optimal strategy, producing a straight-line trajectory to the source. As many surface-adhered bacteria travel in glide-and-reverse patterns[45,46], turning can be especially slow. Thus, in addition to producing the optimal trajectory in a deterministic approximation, the differential strategy would also eliminate the need for sharp trajectory adjustments that would further slow glide-and-reverse bacteria. Future experimental and theoretical work can clarify how microbes actually combine the signals of attractants and repellants to optimize chemotaxis in natural, dynamic environments, as it appears from our work that attraction and repulsion have the potential to combine in surprising and remarkably beneficial ways.

Methods

Point Source Calculation of Spatial Concentrations

For all main text simulations we assumed, for simplicity, a moving point source. We worked in cylindrical coordinates (r, ϕ, z) with the source moving in the $-\hat{z}$ direction along the $r = 0$ z-axis. All scenarios were azimuthally symmetric, allowing us to drop the ϕ component of the coordinate system.

A molecule with diffusion coefficient D_i diffusing from an instantaneous release of a point source at (r, z_{source}) at time will have spatiotemporal concentration

$$c_{\text{inst. Pt.}}(r, z, t | D_i, z_{\text{source}}, t_{\text{release}}) = \frac{1}{\left(4\pi D_i (t - t_{\text{release}})\right)^{3/2}} \exp\left(-\frac{r^2 + (z - z_{\text{source}})^2}{4D_i (t - t_{\text{release}})}\right).$$

If the source is moving downwards at velocity v_{source} and is at the origin (0,0) at time $t = 0$ then it's position as a function of time is $z_{\text{source}}(t) = -v_{\text{source}} t$. The concentration of a molecule continuously diffusing from such as source at time $t = 0$ can then be obtained by integrating over the moving instantaneous point source release:

$$c(r, z | D_i, v_{\text{source}}) = \int_{-\infty}^{0} dt' \; c_{\text{inst. pt.}}(r, z | D_i, -v_{\text{source}} t', t')$$

$$c(r, z | D_i, v_{\text{source}}) = \int_{-\infty}^{0} dt' \; \frac{1}{\left(4\pi D_i (-t')\right)^{3/2}} \exp\left(-\frac{r^2 + (z + v_{\text{source}} t')^2}{4D_i (-t')}\right)$$

$$c(r, z | D_i, v_{\text{source}}) = \frac{1}{4\pi D_i \sqrt{r^2 + z^2}} \exp\left(-\frac{v_{\text{source}}\left(\sqrt{r^2 + z^2} - z\right)}{2D_i}\right)$$

Direction of Motion Under Differential Strategies

Notably, the only component of the log of spatial concentration (calculated above) that is not spherically symmetric around the source's current position is proportional to $1/D_i$:

$$\log[c(r, z | D_i, v_{source})] = \log\left[\frac{1}{4\pi D_i \sqrt{r^2 + z^2}}\right] - \frac{v_{\text{source}}\left(\sqrt{r^2 + z^2} - z\right)}{2D_i}.$$

Thus, weighting a difference of gradient by the ratio of diffusion coefficients can remove any non-spherically symmetric terms, allowing for the simple construction of a differential strategy that always has the microbe swimming directly towards the source.

The generalized differential strategy is a microbe following the gradient of

$$\log[c(r,z|D_{\text{fast}},v_{source})] + \boldsymbol{a}\log[c(r,z|D_{\text{slow}},v_{source})]\ .$$

Unless otherwise specified, "the differential strategy" is the above with $\boldsymbol{a} = -\frac{D_{\text{slow}}}{D_{\text{fast}}}$.

Definitions of Sensing Thresholds and Initial Position

The release rates of both chemoeffectors were assumed to be equal and set such that the concentration of the slow-diffusing chemoeffector at the back end of the source was 1 mM. Sensing thresholds were set to 100 nM for both chemoeffectors. Initial positions were defined in terms of distance from the axis through which the source was traveling. The position parallel to this axis was set based on sensing threshold. For the simulations that became Figures 1-2 as well as Appendix Figures S1-4, the microbe was started at the sensing threshold for the slow-diffusing attractor such it could be assumed to be able to sense both throughout its trajectory towards the source. For the simulations that became Figure 3 as well as Appendix Figures S5-6, the microbe was started at the sensing threshold for the fast-diffusing chemoeffector and could only follow this gradient until reaching the sensing threshold for the slow-diffusing chemoeffector. (Appendix Figure S5) This starting position was chosen for these simulations to most realistically capture the scenario of a microbe attempting to intercept beginning when it would first be able to sense an attractor. The difference in diffusion coefficients meant the slow-diffusing chemoeffector would never be sensed first.

Simulating Trajectories

Except for the explicit run-and-tumble simulations in Appendix §5, trajectories were simulated using a first-order forward Euler method with a sufficiently small time step that further decreases no longer changed the results to within the reported resolutions.

Example Starting Point

When it was considered beneficial to clarity of the figures to show results from a single starting point, we used a point 1850μm from the axis the source is traveling through and 755μm behind the location of the source at the start of the simulation.

Diffusion Coefficients for Amino Acids

Diffusion coefficients came first from linearly extrapolating data in Ma 2005[47] to infinitesimally dilute concentrations. Diffusion coefficients for amino acids not included in Ma came from Miyamoto 2022[48] (specifically the "$_{drv}D_0$" experimentally-based values in Miyamoto's Table 1). The three not included in neither Ma nor Miyamoto's experimental measurements (specifically Cysteine, Glutamine, and Tyrosine) were calculated using equation (3) in Miyamoto 2022 plus an offset of 69 $\mu m^2/s$ (based on the mean difference between values calculated by this equation and the experimentally measured $_{drv}D_0$ values). As Miyamoto had worked at 27.5°C[48,49] whereas Ma had worked at 25°C, all values coming from Miyamoto 2022 were multiplied by (298.2 K)/(300.7 K)=0.991. The complete collection was thus:

	D ($\mu m^2/s$)		D ($\mu m^2/s$)		D ($\mu m^2/s$)		D ($\mu m^2/s$)
Ala	918	Glu	803	Leu	759	Ser	923
Arg	732	Gln	786	Lys	756	Thr	806
Asn	808	Gly	1056	Met	799	Trp	686
Asp	848	His	779	Phe	738	Tyr	727
Cys	842	Ile	772	Pro	832	Val	739

Acknowledgements

We thank the members of the Gore Lab as well as the larger MIT Physics of Living Systems community for their helpful feedback and encouragement to pursue this project.

We acknowledge funding from the Alfred P Sloan Foundation and Schmidt Polymath Award.

We additionally thank the members of the Simons Foundations Principles of Microbial Ecology collaboration for sharing intriguing thoughts and results on marine microbial ecology and the colonization of sinking chitin particles that catalyzed the initial conceptualization of this project.

References

1. Fudickar, A. M., Jahn, A. E. & Ketterson, E. D. Animal Migration: An Overview of One of Nature's Great Spectacles. *Annu. Rev. Ecol. Evol. Syst.* **52**, 479–497 (2021).
2. Stocker, R. Marine microbes see a sea of gradients. *Science* **338**, 628–633 (2012).
3. Fenchel, T. Microbial behavior in a heterogeneous world. *Science* **296**, 1068–1071 (2002).
4. Adler, J. Chemotaxis in Bacteria. *Annu. Rev. Biochem.* (1975).
5. Keegstra, J. M., Carrara, F. & Stocker, R. The ecological roles of bacterial chemotaxis. *Nat. Rev. Microbiol.* **20**, 491–504 (2022).
6. Bi, S. & Sourjik, V. Stimulus sensing and signal processing in bacterial chemotaxis. *Curr. Opin. Microbiol.* **45**, 22–29 (2018).
7. Wong-Ng, J., Celani, A. & Vergassola, M. Exploring the function of bacterial chemotaxis. *Curr. Opin. Microbiol.* **45**, 16–21 (2018).
8. Sourjik, V. & Wingreen, N. S. Responding to chemical gradients: bacterial chemotaxis. *Curr. Opin. Cell Biol.* **24**, 262–268 (2012).
9. Spiro, P. A., Parkinson, J. S. & Othmer, H. G. A model of excitation and adaptation in bacterial chemotaxis. *Proc. Natl. Acad. Sci.* **94**, 7263–7268 (1997).
10. Berg, H. C. & Brown, D. A. Chemotaxis in Escherichia coli analysed by Three-dimensional Tracking. *Nature* **239**, 500–504 (1972).
11. Polin, M., Tuval, I., Drescher, K., Gollub, J. P. & Goldstein, R. E. Chlamydomonas Swims with Two "Gears" in a Eukaryotic Version of Run-and-Tumble Locomotion. *Science* **325**, 487–490 (2009).

12. Adler, J., Hazelbauer, G. L. & Dahl, M. M. Chemotaxis Toward Sugars in Escherichia coli. *J. Bacteriol.* **115**, 824–847 (1973).
13. Mesibov, R. & Adler, J. Chemotaxis Toward Amino Acids in Escherichia coli. *J. Bacteriol.* **112**, 315–326 (1972).
14. Tso, W.-W. & Adler, J. Negative Chemotaxis in Escherichia coli. *J. Bacteriol.* **118**, 560–576 (1974).
15. Benov, L. & Fridovich, I. Escherichia coli exhibits negative chemotaxis in gradients of hydrogen peroxide, hypochlorite, and N-chlorotaurine: products of the respiratory burst of phagocytic cells. *Proc. Natl. Acad. Sci.* **93**, 4999–5002 (1996).
16. Yang, Y. *et al.* Relation between chemotaxis and consumption of amino acids in bacteria. *Mol. Microbiol.* **96**, 1272–1282 (2015).
17. Oosawa, K. & Imae, Y. Glycerol and ethylene glycol: members of a new class of repellents of Escherichia coli chemotaxis. *J. Bacteriol.* **154**, 104–112 (1983).
18. Dowdell, A., Paschke, P. I., Thomason, P. A., Tweedy, L. & Insall, R. H. Competition between chemoattractants causes unexpected complexity and can explain negative chemotaxis. *Curr. Biol.* **33**, 1704-1715.e3 (2023).
19. Oliveira, N. M. *et al.* Suicidal chemotaxis in bacteria. *Nat. Commun.* **13**, 7608 (2022).
20. Yang, J. *et al.* Biphasic chemotaxis of Escherichia coli to the microbiota metabolite indole. *Proc. Natl. Acad. Sci.* **117**, 6114–6120 (2020).
21. Kalinin, Y., Neumann, S., Sourjik, V. & Wu, M. Responses of Escherichia coli Bacteria to Two Opposing Chemoattractant Gradients Depend on the Chemoreceptor Ratio. *J. Bacteriol.* **192**, 1796–1800 (2010).
22. Strauss, I., Frymier, P. D., Hahn, C. M. & Ford, R. M. Analysis of bacterial migration: II. Studies with multiple attractant gradients. *AIChE J.* **41**, 402–414 (1995).
23. Park, J. & Aminzare, Z. A Mathematical Description of Bacterial Chemotaxis in Response to Two Stimuli. *Bull. Math. Biol.* **84**, 9 (2021).
24. Adler, J. & Tso, W.-W. 'Decision'-Making in Bacteria: Chemotactic Response of Escherichia coli to Conflicting Stimuli. *Science* **184**, 1292–1294 (1974).
25. Livne, N. & Vaknin, A. Collective responses of bacteria to a local source of conflicting effectors. *Sci. Rep.* **12**, 4928 (2022).

26. Zhao, X. & Ford, R. M. Escherichia coli chemotaxis to competing stimuli in a microfluidic device with a constant gradient. *Biotechnol. Bioeng.* **119**, 2564–2573 (2022).
27. Zhao, X. & Ford, R. M. Marine Bacteria Chemotaxis to Crude Oil Components with Opposing Effects. 2022.01.26.477900 Preprint at https://doi.org/10.1101/2022.01.26.477900 (2022).
28. Middlebrooks, S. A., Zhao, X., Ford, R. M. & Cummings, P. T. A mathematical model for Escherichia coli chemotaxis to competing stimuli. *Biotechnol. Bioeng.* **118**, 4678–4686 (2021).
29. Englert, D. L., Manson, M. D. & Jayaraman, A. Flow-Based Microfluidic Device for Quantifying Bacterial Chemotaxis in Stable, Competing Gradients. *Appl. Environ. Microbiol.* **75**, 4557–4564 (2009).
30. Narla, A. V., Cremer, J. & Hwa, T. A traveling-wave solution for bacterial chemotaxis with growth. *Proc. Natl. Acad. Sci.* **118**, e2105138118 (2021).
31. Cremer, J. *et al.* Chemotaxis as a navigation strategy to boost range expansion. *Nature* **575**, 658–663 (2019).
32. Nguyen, T. T. H. *et al.* Microbes contribute to setting the ocean carbon flux by altering the fate of sinking particulates. *Nat. Commun.* **13**, 1657 (2022).
33. Stocker, R., Seymour, J. R., Samadani, A., Hunt, D. E. & Polz, M. F. Rapid chemotactic response enables marine bacteria to exploit ephemeral microscale nutrient patches. *Proc. Natl. Acad. Sci.* **105**, 4209–4214 (2008).
34. Alldredge, A. L. & Gotschalk, C. In situ settling behavior of marine snow. *Limnol. Oceanogr.* **33**, 339–351 (1988).
35. Alldredge, A. L. & Gotschalk, C. C. Direct observations of the mass flocculation of diatom blooms: characteristics, settling velocities and formation of diatom aggregates. *Deep Sea Res. Part Oceanogr. Res. Pap.* **36**, 159–171 (1989).
36. Słomka, J., Alcolombri, U., Secchi, E., Stocker, R. & Fernandez, V. I. Encounter rates between bacteria and small sinking particles. *New J. Phys.* **22**, 043016 (2020).
37. Roberts, E. C., Legrand, C., Steinke, M. & Wootton, E. C. Mechanisms underlying chemical interactions between predatory planktonic protists and their prey. *J. Plankton Res.* **33**, 833–841 (2011).

38. Hartz, A. J., Sherr, B. F. & Sherr, E. B. Using Inhibitors to Investigate the Involvement of Cell Signaling in Predation by Marine Phagotrophic Protists. *J. Eukaryot. Microbiol.* **55**, 18–21 (2008).
39. Walsh, F. & Mitchell, R. Bacterial chemotactic responses in flowing water. *Microb. Ecol.* **4**, 165–168 (1977).
40. Galilei, G. *Dialogo sopra i due massimi sistemi del mondo*. (1632).
41. Grognot, M. & Taute, K. M. A multiscale 3D chemotaxis assay reveals bacterial navigation mechanisms. *Commun. Biol.* **4**, 1–8 (2021).
42. Kiørboe, T., Ploug, H. & Thygesen, U. H. Fluid motion and solute distribution around sinking aggregates. I. Small-scale fluxes and heterogeneity of nutrients in the pelagic environment. *Mar. Ecol. Prog. Ser.* **211**, 1–13 (2001).
43. Krishnamurthy, D., Pepper, R. & Prakash, M. Active sinking particles: sessile suspension feeders significantly alter the flow and transport to sinking aggregates. *J. R. Soc. Interface* **20**, 20220537 (2023).
44. Chajwa, R., Flaum, E., Bidle, K. D., Van Mooy, B. & Prakash, M. Hidden Comet-Tails of Marine Snow Impede Ocean-based Carbon Sequestration. Preprint at https://doi.org/10.48550/arXiv.2310.01982 (2023).
45. McBride, M. J. Bacterial Gliding Motility: Multiple Mechanisms for Cell Movement over Surfaces. *Annu. Rev. Microbiol.* **55**, 49–75 (2001).
46. Harshey, R. M. Bacterial Motility on a Surface: Many Ways to a Common Goal. *Annu. Rev. Microbiol.* **57**, 249–273 (2003).
47. Ma, Y., Zhu, C., Ma, P. & Yu, K. T. Studies on the Diffusion Coefficients of Amino Acids in Aqueous Solutions. *J. Chem. Eng. Data* **50**, 1192–1196 (2005).
48. Miyamoto, S., Ekino, K. & Shimono, K. Estimation of the Diffusion Coefficients of Small Molecules by Diffusion Measurements with Agar-gel and Theoretical Molecular Modeling. *Chem-Bio Inform. J.* **22**, 13–20 (2022).
49. Miyamoto, S., Atsuyama, K., Ekino, K. & Shin, T. Estimating the Diffusion Coefficients of Sugars Using Diffusion Experiments in Agar-Gel and Computer Simulations. *Chem. Pharm. Bull. (Tokyo)* **66**, 632–636 (2018).

Appendix

§1 Additional Information Supplementing Figures 1 and 2

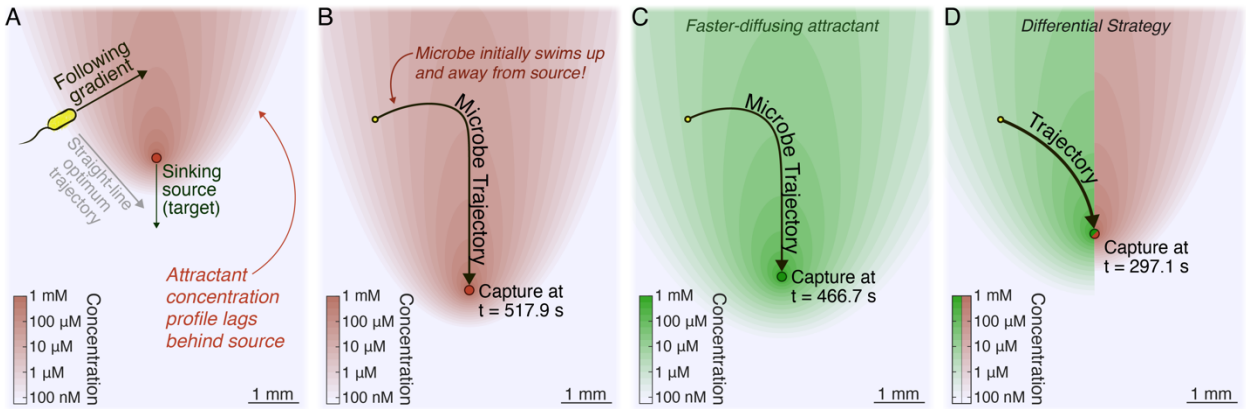

Appendix Figure S1. (**A**) Same as Fig 1B (including with the microbe in the same example location) but for the D = 500 μm²/s chemoeffector. Specifically, concentration profile of a molecule with diffusion coefficient 500 μm²/s being released from source moving downwards at 5 μm/s. The arrow labeled "Following gradient" indicates the direction of the gradient of the concentration at an example point at the center of the microbe's body. Light grey arrow shows the direct the microbe should ideally traveling in (assuming a swim speed of 10 μm/s) to most efficiently intercept the particle. (This light gray arrow is the same as the arrow labeled "(Ideal)" in Fig 1C.) (**B**) Same as Fig 1C but for the D = 500 μm²/s chemoeffector. Specifically, trajectory that a microbe starting at the example point in **A** would follow to intercept the moving source if it followed the gradient of the D = 500 μm²/s chemoeffector. Drawn in the same stationary frame as **A** at the moment the source is intercepted. (**C**) Same trajectory as Fig 1C reproduced here to facilitate direct comparison. Specifically, same as **B** but for a chemoeffector with diffusion coefficient of 1000 μm²/s. (**D**) Same trajectory as Fig 2D reproduced here to facilitate direct comparison. Specifically, the trajectory produced by the differential strategy with the microbe starting at the same example point as in **A-C**.

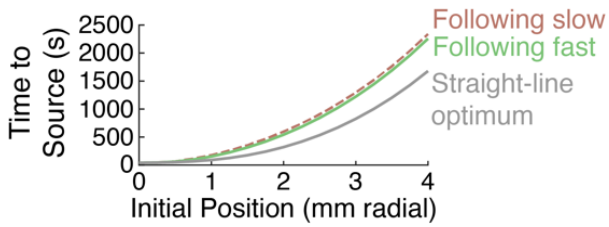

Appendix Figure S2. Time to source for a microbe following the gradient of the slow or fast diffusing chemoeffector with the time to source if the microbe could follow an optimal straight-line trajectory shown for comparison. Initial position is distance radially from the axis the source is traveling through. Position parallel to this axis is set such that the concentration of the slow-diffusing attractant at the starting location is 100 nM (Methods).

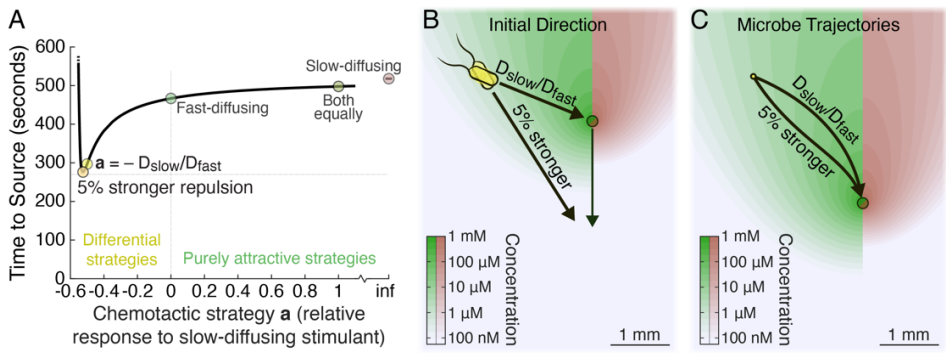

Appendix Figure S3. (**A**) Same plot as Fig 2E reproduced here for easy reference. Specifically, time to reach the source when starting at the same example point used in Fig 1, Fig 2D-E, and Appendix Fig S1 for a generalization of differential strategy in which the relative response to the slow-diffusing chemoattractant is now a function of variable $\boldsymbol{a}$. Vertical dashed line separates the different strategies in which the slow-diffusing chemoeffector is used as a repellant (negative $\boldsymbol{a}$) from the strategies in which both chemoeffectors are attractants (positive $\boldsymbol{a}$). Horizontal dashed line represents the fastest the microbe could possibly reach the source if it could follow any straight-line trajectory. (**B**) For the same example point, comparison of the initial direction a microbe following the default differential strategy $\boldsymbol{a} = -\frac{D_{\text{slow}}}{D_{\text{fast}}}$ or the strategy with 5% stronger repulsion $\boldsymbol{a} = -1.05\frac{D_{\text{slow}}}{D_{\text{fast}}}$ would be traveling in. (**C**) Trajectories for those two strategies.

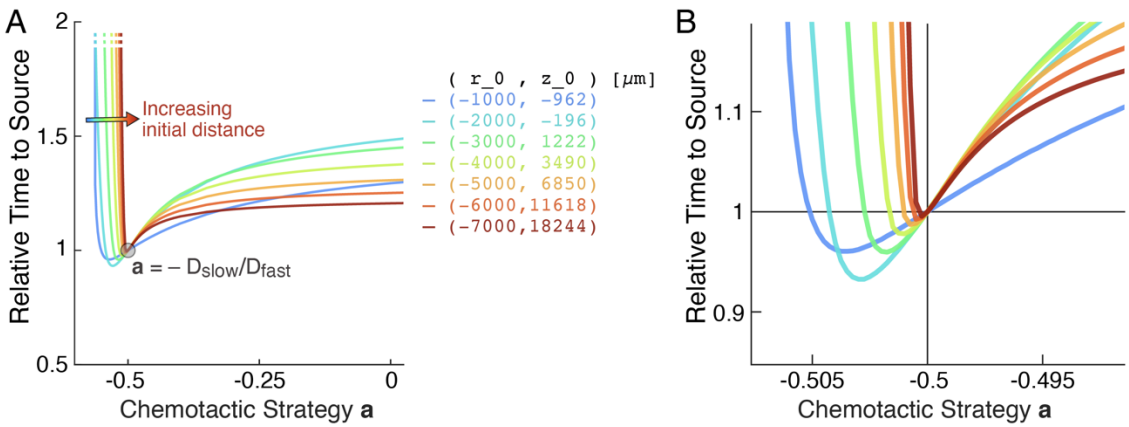

Appendix Figure S4. (**A**) Same as in Fig 2E and Appendix Fig S3A but with each line representing results from using a different initial position. Time to source is normalized to the value for $\boldsymbol{a} = -\frac{D_{\text{slow}}}{D_{\text{fast}}}$. (**B**) Zoom in on the most relevant region in **A**.

§2 Illustration of Scenario Simulated in Figure 3B

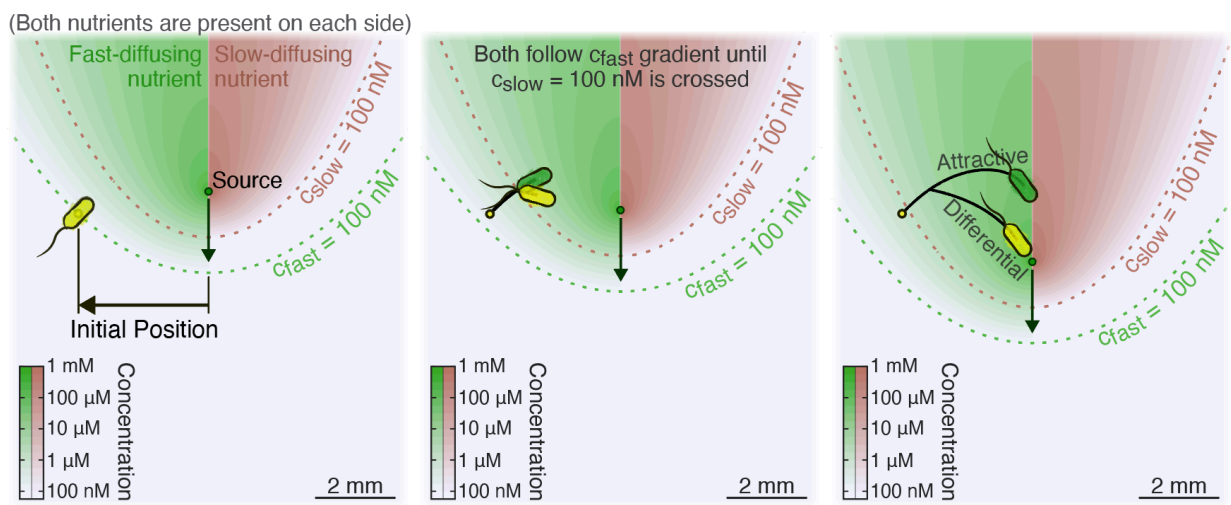

Appendix Figure S5. Illustration of the scenario simulated to determine reduction in time-to-source as a function of initial position and velocity ratio (the results shown in Fig 3B). Left panel shows how initial position is defined such that the microbe starts at a point where the concentration of the fast-diffusing attractant is 100 nM (Methods). Middle panel illustrates how regardless of strategy, the microbe will follow the gradient of the fast-diffusing attractant until it reach the region where the concentration of the slow-diffusing attractant is greater than 100 nM. Right panel illustrates the trajectories under the two strategies then diverging.

§3 Quantifying the Likelihood of Intercepting Faster-Moving Source

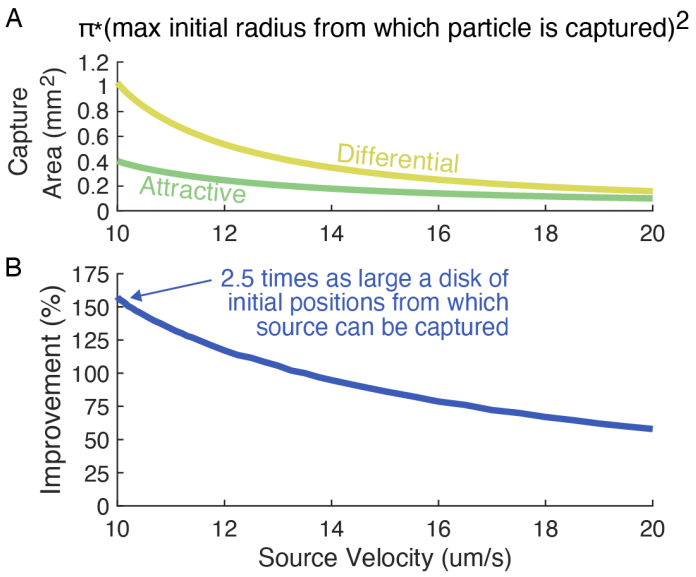

Appendix Figure S6. (**A**) Area of initial positions from which a microbe swimming at 10 μm/s following the purely attractive or differential strategy could intercept a particle of radius 100 μm when the available attractants have diffusion coefficients of 500 $\mu m^2/s$ and 1000 $\mu m^2/s$. This capture area equals π time the square of the maximum initial radial position from which the particle can be captured and is proportionally to the number of microbes that would intercept the particle if they were uniformly distributed in space and remained stationary until the local concentrations of one of the attractant exceeded 100 nM (Methods). (**B**) Increase in capture area for the differential strategy as compared to the purely attractive strategy.

§4 Model of *E. coli* Tsr Receptors and CheA-Mediated Response

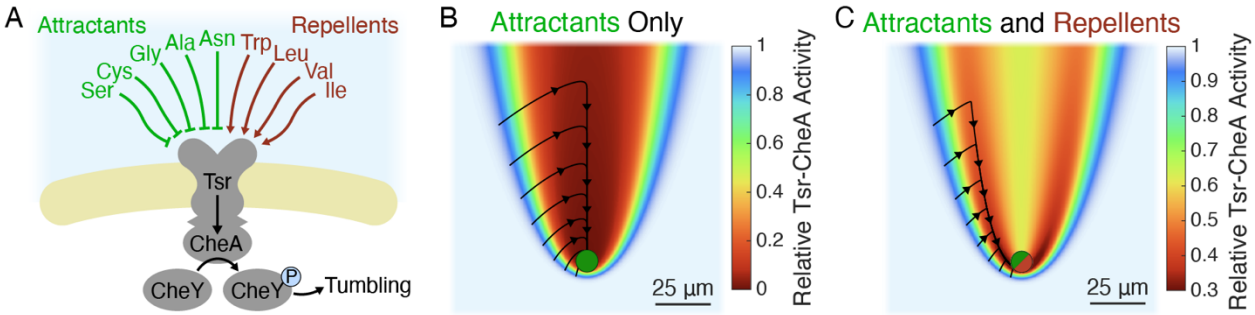

Appendix Figure S7. (**A**) Visual depiction of our simplified model of *E. coli*'s chemotactic response to amino acids. We simplify by including on the Tsr receptor and assume competitive ligand binding. The attractants inhibit the Tsr-CheW-CheA complex while the repellents increase its activity. CheA phosphorylates CheY, which in turn promotes tumbling. Not explicitly modeled is methylation of the Tsr receptor, which helps prevent saturation of the response. Thus *E. coli*'s becomes more likely to tumble and reorient itself as attractant concentrations decrease and repellents concentration increase and, after averaging over many runs and tumbles, will follow gradients of decreasing CheA activity. (**B**) Trajectories following a decreasing gradient of CheA activity when the five attractants are being released from the source using parameters in Appendix Table S1. (**C**) Trajectories following a decreasing gradient of CheA activity when the attractants and repellents are being released from the source. The presence of the repellents decreases the time to source by 22% on average.

	Diffusion coefficient ($\mu m^2/s$)	Tsr-AA equilibrium coefficient (μM)	Relative Tsr activity at saturation
Serine	923	$10^{-1.03}$	0
Cysteine	842	$10^{0.88}$	0
Glycine	1056	$10^{1.56}$	0
Alanine	918	$10^{1.74}$	0
Asparagine	808	$10^{1.83}$	0
unbound Tsr	n/a	n/a	1
Tryptophan	686	$10^{2.36}$	2.38
Leucine	759	$10^{4.95}$	4.95
Valine	739	$10^{3.22}$	3.22
Isoleucine	772	$10^{3.50}$	3.50

Appendix Table S1. Parameters used to calculate CheA activity. Diffusion coefficients are sources as described in the Methods. Tsr properties are extracted SI Figures S2B and S10C of Yang 2015[16].

§5 Simulations with Explicit Run-and-Tumble Motion

In the Main Text, we considered a deterministic model in which the microbe can exactly follow the concentration gradient. However, microbes usually navigate with a run-and-tumble motion or some similar varition, so here we consider those dynamics and test whether the repulsion from slow-diffusing nutrients still improves chemotaxis under this extension.

We modeled the run-and-tumble motion by assuming that the microbe is more likely to tumble and reorient its movement when the environment is worsening. When there is only attractant, the environment is considered improving when the local concentration of attractant increases. In the presence of both attractant and repellent, the environment is considered improving when $\log[c_{fast}] - \frac{D_{slow}}{D_{fast}}\log[c_{fast}]$ at the microbe's (moving) position is increasing.

In our stochastic simulation, this chemotactic run-and-tumble motion is implemented by using two different tumbling rates depending on whether the environment is improving or worsening as the microbe runs. Specifically, as the simulation proceeds with each time-step dt, microbe runs by $v_{run}dt$ in the direction it is facing, then checks whether the environment has improved or worsen over the time-step. The microbe has either $P_1 dt$ (if environment has improved) or $P_2 dt$ (if environment has worsened) chance to tumble and choose a new random direction. Specifically, if a random number $\text{Uniform}(0,1) < P_i dt$, the microbe tumbles; otherwise, it keeps running in the same direction. In addition, as we consider the co-moving frame of the source, microbe drifts by $v_{\text{source}}dt$ in $+z$ direction. This run-and-tumble motion continues until the microbe intercepts the source by coming within 100 μm. We use $dt = 10\ ms$, and the results are robust under any sufficiently small dt.

We chose tumbling rates $P_1 = 0.2/s$ when the environment improves and $P_2 = 5/s$ when the environment worsens. We used the run speed of microbe $v_{run} = 20\ \mu m/s$, which led to average speed over a constant gradient $v_{microbe} \simeq 10\ \mu m/s$. All other parameter choices followed the main text: $v_{source} = 5\ \mu m/s$, $D_{fast} = 1000\ \mu m^2/s$, $D_{slow} = 500\ \mu m^2/s$, and $a = -D_{slow}/D_{fast} = -0.5$.

In Fig. S8, we show the statistics (over 1000 simulations) of the time it took for microbes to reach the source with initial distance 5 mm away. As in the deterministic chemotaxis, the run-and-tumble chemotaxis is improved with repulsion from slow-diffusing nutrient, taking almost half the time to capture the moving source compared to attractant-only case.

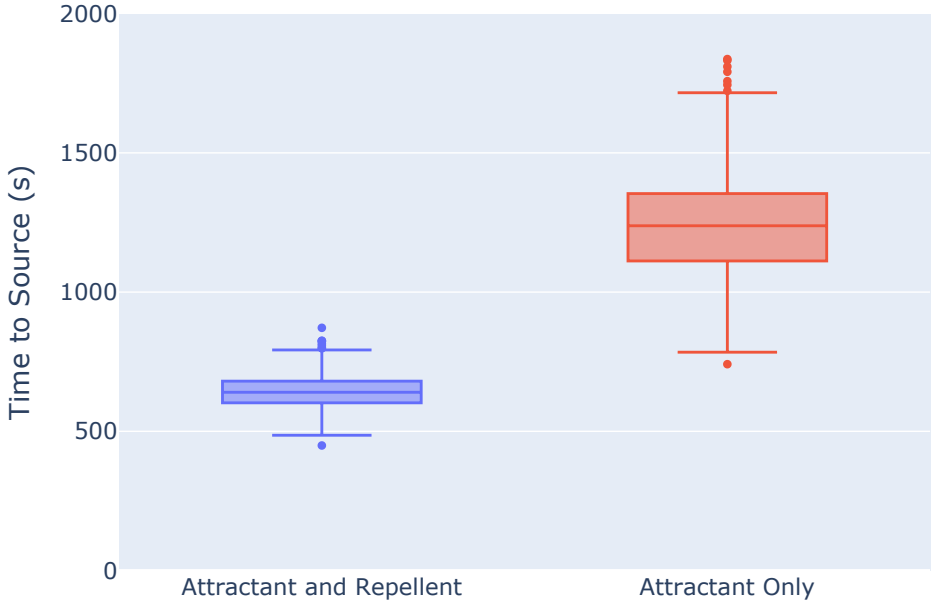

Appendix Figure S8. Time to reach the source under run-and-tumble chemotaxis. "Attractant and Repellent" strategy took 641.5 ± 59.1 s (SD, N=1000), while "Attractant Only" strategy took 1239.7 ± 185.3 s (SD, N=1000).